Evaluation of adsorptive and synergistic effects for elimination of crystal violet from aqueous solution

Dilek Gümüş

Sinop University, Directorate of Construction and Technical Works, 57010 Sinop, Turkey; email: dilek.gumus@gmail.com

ABSTRACT

This study investigated removal of crystal violet (CV) from aqueous solutions by iron oxide-coated zeolite (ICZ), potassium permanganate-coated zeolite (MCZ), and zero-valent iron (ZVI) and evaluated synergistic effect of sequential system. The adsorbents were characterized using energy-dispersive X-ray analysis and scanning electron microscopy images. The effects of various parameters were examined. The results showed that basic pH generally favored adsorption for ICZ and MCZ but significant CV removal was possible even under neutral conditions. ICZ and MCZ exhibited the best performance at pH 11. ZVI displayed the best performance at pH 7, and the adsorption was very fast. The experimentally obtained data for the adsorption of CV onto ICZ, MCZ, and ZVI were modeled using the isotherm models of Freundlich and Langmuir. The kinetics of CV onto ICZ, MCZ, and ZVI was best described by the pseudo-second-order kinetic model. This study reveals that it is possible to use ICZ, MCZ, and ZVI as nanoparticles, an alternative for the adsorbents that are already being used, in the removal of CV from industrial wastewater. Furthermore, the combination of ZVI and MCZ enhances the decolorization of the solutions. The best result was found with the ZVI-MCZ sequential system.

Keywords: Adsorption; Iron oxide-coated zeolite; Potassium permanganate-coated zeolite; Zero-valent iron; Kinetics; Isotherm; Synergic effect

1. Introduction

Wastewater effluents that come from many industries such as paper, textile, rubber, leather, plastics, cosmetic, and printing industries, contain several kinds of synthetic dyestuffs [1]. The discharges of coloring industries into the hydrosphere constitute an important source of pollution due to their recalcitrant nature. This gives an undesirable color to the water body, which reduces sunlight penetration and hinders resistance to photochemical and biological attacks on aquatic life. In up-to-date data, more than 100,000 commercial dyes are known with a production of over 7×10^5 ton/year. The total dye consumption in the textile industry worldwide is more than 10,000 ton/year, and approximately 100 ton/year of dyes is discharged into water streams [2]. Dyes are considered an objectionable type of pollutant, because they are generally toxic when ingested or inhaled and lead to problems such as skin and eye irritation, and skin sensitization, which might also be due to carcinogenicity. They provide color to

water, which is visible to human eye, and therefore they are highly objectionable on esthetic grounds [3].

Crystal violet (CV), a member of the triphenylmethane group, is a basic cationic synthetic dye and creates a violet color in aqueous solution. Cationic dyes are more toxic than the anionic dyes [4]. It is widely used in textile dyeing industries, as a biological stain, as a dermatological agent, in veterinary medicine, and as an additive to poultry feed to inhibit propagation of harmful bacteria, parasites, and fungi. However, CV is also a mutagenic, carcinogenic, and mitotic poison [5] and a proven recalcitrant molecule.

Various methods such as adsorption [6], coagulation, electrocoagulation [7], membrane separation [8], and advanced oxidation [9] are used in removal of dyes from wastewater. Adsorption is one of the most effective processes of advanced wastewater treatment, which industries employ to reduce hazardous inorganic/organic pollutants present in the effluent [2]. Some natural materials such as zeolites, chitosan, and clay are being considered as alternative low-cost adsorbents.

Because their sorption capacity is usually less than that of synthetic or modified adsorbents, to enhance the sorption capacity of natural adsorbents to adsorb heavy metals, many attempts have been made including chemical modification of their surface using metal oxides [10]. Several researchers have studied the adsorption behavior of zeolites [11–13]. However, natural zeolite was not suitable for removal of dyes due to their extremely low sorption capacities [2]. Previous studies have attempted physicochemical methods and various modification approaches such as acid pretreatment, surfactant modification, and thermal activation on natural zeolite for the enhanced adsorption [14,15]. All these studies have indicated considerably favorable results in terms of enhancing the adsorption performance of natural zeolite. The reason for choosing manganese oxide and iron oxide as support materials is that Fe or Mn oxides have a relatively higher affinity for cations [16,17]. Adsorption of CV onto manganese oxide-coated sepiolite has been studied by Eren et al. [18]. Adsorption of methylene blue (MB) and methyl orange onto zeolite and iron oxide-coated zeolite (ICZ) was reported. The adsorption capacity of ICZ was higher than that of zeolite [19,20]. To the best of the author's knowledge, adsorptions of CV by ICZ, potassium permanganate-coated zeolite (MCZ), and zero-valent iron (ZVI) have not been studied.

The aim of this study is to examine the effectiveness of ICZ, MCZ, and ZVI in removing CV from aqueous solutions and compare the adsorption capacity of different adsorbents. Moreover, the efficiency of a ZVI-MCZ combined system is investigated in removing CV from an aqueous solution.

2. Material and methods

2.1. Chemicals

All the chemicals provided by Sigma-Aldrich (Germany) were of analytical grade. A stock solution of CV of 1,000 mg/L was prepared and diluted to the required initial concentrations. Dye solutions were prepared by deionized water. Initial and residual concentrations of CV were determined by a UV–visible spectrophotometer (Thermo GENESYS 10 UV-Vis spectrophotometer) at 590 nm (λ_{max}). The pH values of the dye solutions were adjusted by adding HCl (0.1N) or NaOH (0.1N) solutions using a pH meter (Eutech CyberScan PC 500). The pH values at the point of zero charge (pH_{pzc}) for ICZ and MCZ samples were determined through a pH equilibration method [21]. Scanning electron microscopy (SEM) and energy-dispersive X-ray (EDX) analyses were performed by SEM (QUANTA 400F Field Emission SEM) and VEGA II XMU.

2.2. Preparation of ICZ

The zeolite (clinoptilolite) samples that were used in this study were received from the Göhrde region in Manisa, Turkey. The raw sample was ground by a primary crusher (hammer-type), and then sieved to +45 −35 mesh particle-size pieces. These were coated by iron using reagent grade FeCl$_3$.6H$_2$O, employing the method reported by Lai and Chen [2], Lai et al. [23], and Kitis et al. [24]. For modification, 50 g of zeolite was first kept in an HCl (1 N) solution at pH 1, for 24 h at room temperature, rinsed with distilled (DI) and

deionized water several times, and then dried at 105°C for 24 h. The dried zeolite sample was placed in a glass flask, and solution of 0.5 M Fe (III) was added until all zeolite was soaked in the solution. While combining the mixture, NaOH (3 N) was added dropwise until pH 9.5 is reached. After pH adjustment, the mixture was stirred at high speed for 5 min, mixed in a temperature-controlled shaker at 60°C ± 1°C and 150 rpm for about 24 h, and then dried at 105°C ± 1°C for 24 h. The dried material was washed 4–5 times and dried again at 60°C ± 1°C for 24 h. The coated zeolites were kept in closed polyethylene bottles at room temperature in dark [25].

2.3. Preparation of MCZ

The MCZ was prepared as follows: Prior to the coating treatment, the zeolite was converted to its Na form by suspending 30 g of zeolite in 500 mL of 1 M NaCl solution for 24 h. The zeolite suspension was filtered and washed with deionized water. The resulting Na–zeolite was dried in an oven at 100°C for 24 h before use [26]. The MCZ was prepared utilizing a modified reductive procedure to precipitate colloids of manganese oxides onto Na–zeolite surfaces. Manganese oxide was precipitated in the aqueous solution by the following reaction:

$$2KMnO_4 + 8HCl \rightarrow 2MnO_2 + 2KCl + 3Cl_2 + 4H_2O \qquad (1)$$
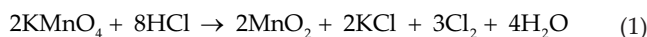
The dried Na–zeolite samples were added into a beaker containing a heated solution of potassium permanganate at 90°C. A volume of hydrochloric acid (37.5%, $W_{HCl} = W_{H2O}$) was added dropwise to the mixture. After stirring for 1 h, the suspension was filtered, washed several times using DI water (to remove free potassium and chloride ions), dried in an oven at 100°C for 24 h, and stored in polyethylene bottles for further use [27].

2.4. Preparation of ZVI

Nano iron was prepared as described by Wang et al. [28]. ZVI was prepared by adding 100 mL of 2.5 M KBH$_4$ solution dropwise into 200 mL 0.5 M FeSO$_4$ solution with vigorous magnetic stirring at 150 rpm. The solution was stirred for additional 10 min after KBH$_4$ was completely added into the FeSO$_4$ solution. ZVI could be synthesized according to the following reaction:

$$Fe^{2+} + 2BH_4^- + 6H_2O \;\rightarrow\; Fe^0\downarrow \;+\; 2B(OH)_3 + 7H_2\uparrow$$

$$(2)$$
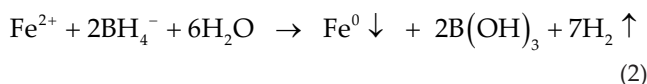
The obtained ZVI particles were rinsed three times with DI water and absolute ethanol, and dried in a vacuum drying oven at room temperature. The prepared ZVI was then stored in vials for further characterization and the adsorption experiments.

2.5. Batch adsorption experiments

Batch adsorption experiments were conducted to investigate the effects of various parameters such as contact

time, dye concentration, adsorbent dosage, and pH on dye solution adsorption. Batch experiments were performed for different dye concentrations (50–250 mg/L), pH (3–11), adsorbent doses (0.5–10 g/L), and contact times (0–200 min). After the prescribed contact time, in the ICZ, MCZ, and ZVI experiments, the solution was centrifuged and the final concentration of dye solution was measured using UV–visible spectrophotometer.

For each adsorption isotherm, an experiment was conducted at equilibrium time. The adsorption capacities (q_t and q_e, mg/g) were calculated by the following equations:

$$q_e = \frac{(C_0 - C_e).V}{m} \tag{3}$$

$$q_t = \frac{(C_0 - C_t).V}{m} \tag{4}$$

where q_t and q_e are the amounts of dye adsorbed (mg/g) at time t and equilibrium time, respectively, C_0, C_t, and C_e (mg/L) are the initial, t time, and equilibrium concentrations of dye in solution, respectively, V (L) is the volume of the dye solution, and m (g) is the mass of the adsorbent.

To find the equilibrium time for sorption of CV on the adsorbents, a known dosage of the adsorbent was mixed with 100 mL of CV 100 mg/L solutions separately and adjusted to the desired pH. The solutions were shaken with a shaker for different time intervals from 0 to 200 min. All experiments were performed within the equilibrium times.

Isotherm modeling studies were performed using adsorbent masses of 1 g/L in solutions of varying concentrations (50–250 mg/L) for a period equal to the equilibrium time for ICZ and ZVI. It was performed using adsorbent masses of 0.5 g/L in solutions of varying concentrations (50–250 mg/L) for MCZ. Kinetic and isotherm studies were performed by determining the optimum experimental conditions [18].

3. Results and discussion

3.1. Characterization of adsorbents

The SEM images of natural zeolite, ICZ, MCZ, and ZVI are shown in Figs. 1(a)–(d), respectively. The surface morphologies of the adsorbents after the adsorption processes are shown in Figs. 1(e)–(g), respectively. The samples of ICZ were dark red-colored precipitates, indicating the presence of iron in the form of insoluble oxides. The samples of MCZ were dark grey-colored precipitates, indicating the presence of manganese.

The ICZ and MCZ surfaces were apparently occupied by newborn iron oxides and manganese oxides, respectively, which were formed during the coating process. Figs. 1(b) and (c) also show iron and manganese oxides formed in clusters, apparently on occupied surfaces. Iron and manganese oxide coatings were composed of small particles on top of natural zeolite on the micron scale. Zeolites are naturally negatively charged and have high ion-exchange capacity. However, due to the positive charge of the oxide-covering layer [29], surface properties of zeolite have changed. This result indicated
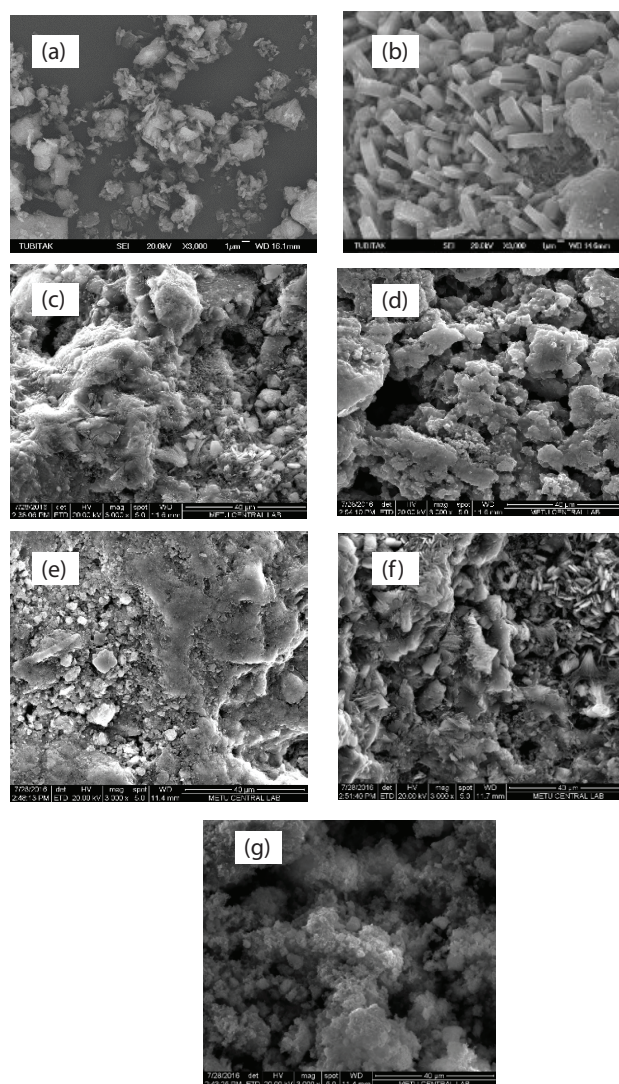

Fig. 1. SEM images of the adsorbents: (a) natural zeolite, (b) ICZ, (c) MCZ, (d) ZVI, (e) ICZ-CV, (f) MCZ-CV, and (g) ZVI-CV.

that the micropores and mesopores on zeolite, which might promote colorant adsorption, were occupied by manganese and iron oxides. These surfaces were covered with colorant molecules after the adsorption as shown in Figs. 1(e)–(g).

EDX analysis yielded direct evidence for iron oxide and manganese oxide coated on the surface of zeolite. EDX results of natural zeolite, ICZ, and MCZ were given in Table 1.

3.2. Effect of contact time

In order to determine the effect of contact time, the adsorption process was studied in the time range from 0 to 200 min at a colorant concentration of 50 mg/L with a fixed adsorbent amount (2 g/L), at pH 6.45 (the native PH of the solution) for ICZ, MCZ, and ZVI. On the other hand, the time range from 0 to 120 min was studied with a fixed adsorbent amount (2 g/L) for ZVI. The adsorption capacities of CV increased with an increase in contact time. Figs. 2(a) and (b) show that the adsorptions onto ICZ and MCZ were fast for the first 90 min and equilibriums were reached within

180 and 150 min., respectively. Dye removal was achieved within 30 min for ZVI, and there was no significant change in residual CV concentrations after this time up to 120 min. The adsorption onto ZVI-CV proceeded fast within the first 5 min, and then slowed down and reached equilibrium. The possible reason is that in the initial phase, CV dye molecules could easily be transported to the surface of ZVI particles because of the strong adsorption ability of ZVI. The results are consistent with those observed by Sarma et al. [30].

Table 1
EDX results of natural zeolite, ICZ, and MCZ

Elements	Zeolite (%)	Iron oxide-coated zeolite (ICZ) (%)	Potassium permanganate-coated zeolite (MCZ) (%)
Al	8.16	5.16	6.91
Fe	0.78	11.88	2.97
K	2.96	1.11	7.28
Mn	0.02	0.12	4.6
Na	0.71	1.16	0.73
O	49.97	48.51	43.08
Si	37.40	32.06	34.43

3.3. Effect of adsorbent dose

One of the parameters affecting the adsorption process is the amount of the adsorbent. In order to investigate the effect of the doses of ICZ, MCZ, and ZVI on CV removal, a series of adsorption doses was applied at an initial CV concentration of 50 mg/L, pH 6.45, and in equilibrium time.

The effects of ICZ and MCZ doses ranging from 0.5 to 10 g/L and the effects of ZVI doses ranging from 0.5 to 5 g/L on CV removal efficiencies and sorption capacities are illustrated in Figs. 3(a) and (b).

The removal of CV increased from 56.24% to 99.57% for ICZ doses of 0.5–10 g/L. The removal of CV increased from 87.06% to 99.81% for MCZ doses of 0.5–10 g/L. Moreover, the removal of CV increased from 38.57% to 96.27% for ZVI dose of 0.5–1 g/L. Then, the removal of CV decreased from 96.27% to 69.01% for ZVI doses of 1–5 g/L.

As seen in Fig. 3(a), the removal efficiencies rose with increasing adsorbent doses, where the quantity of sorption sites at the surface of adsorbent increased by increasing the amount of the adsorbent for ICZ and MCZ [2]. Additionally, for ZVI, the removal efficiency increased up to 1 g/L and then decreased with increasing adsorbent dosage. At higher adsorbent dosage, the potential aggregation of ZVI particles limited the adsorption efficiency of ZVI [31], and it may be seen in Fig. 3(b) that the adsorption capacity of CV increased up to 1 g/L but became almost constant till 3 g/L, and then the amount of CV adsorbed per unit mass of the adsorbent
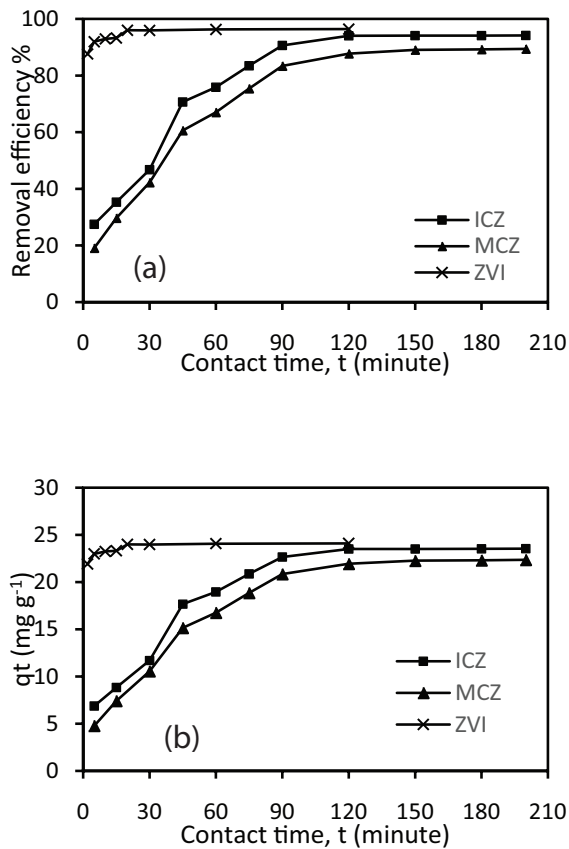

Fig. 2. Effect of contact time on the adsorption of CV on ICZ, MCZ, and ZVI: (a) removal efficiency and (b) adsorption capacity (optimum parameters: C_0, 50 mg/L; adsorbent dosage, 2 g/L; initial pH, 6.45; and agitation speed, 150 rpm).
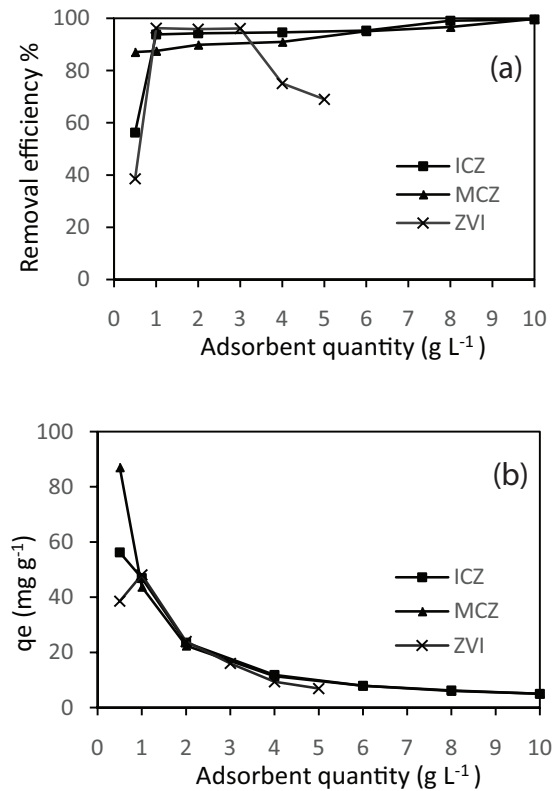

Fig. 3. Effect of adsorbent quantity on the adsorption of CV on ICZ, MCZ, and ZVI: (a) removal efficiency and (b) adsorption capacity (optimum parameters: C_0, 50 mg/L; initial pH, 6.45; and agitation speed, 150 rpm).

decreased very sharply with increases in the adsorbent dosages for ZVI. The adsorption capacity of CV on ICZ decreased with increase in the adsorbent dosages, but this decline was very sharp in the adsorbent dosage range of 1–10 g/L. The adsorption capacity of CV on MCZ remained almost constant at concentrations of 0.5 and 1 g/L and decreased after 1 g/L.

The decrease in the amount of adsorbed dye, q_e (mg/g), with increasing adsorbent mass is due to the split in the flux or the concentration gradient between the solute concentration in the solution and the solute concentration in the surface of the adsorbent [1]. The effect of adsorbent dosage provides an idea for the ability of a dye to be adsorbed with the smallest amount of adsorbent, to recognize the capability of a dye from an economic point of view [2]. Therefore, the optimum amount of the adsorbents (ICZ and ZVI) was found as 1 g/L. The optimum amount of MCZ was found as 0.5 g/L. At the optimum amounts of the selected adsorbents, the adsorption capacity for CV was found as 46.93, 87.06, and 48.13 mg/g in ICZ, MCZ, and ZVI, respectively.

3.4. Effect of solution pH

The pH_{pzc} of ICZ, MCZ, and ZVI was measured as 4.02 ± 0.2, 3.12 ± 0.2, and 5.1, respectively. The effects of initial solution pH on CV adsorption onto the adsorbents were studied within the pH range of 3–11 at equilibrium time as shown in Figs. 4(a) and (b).
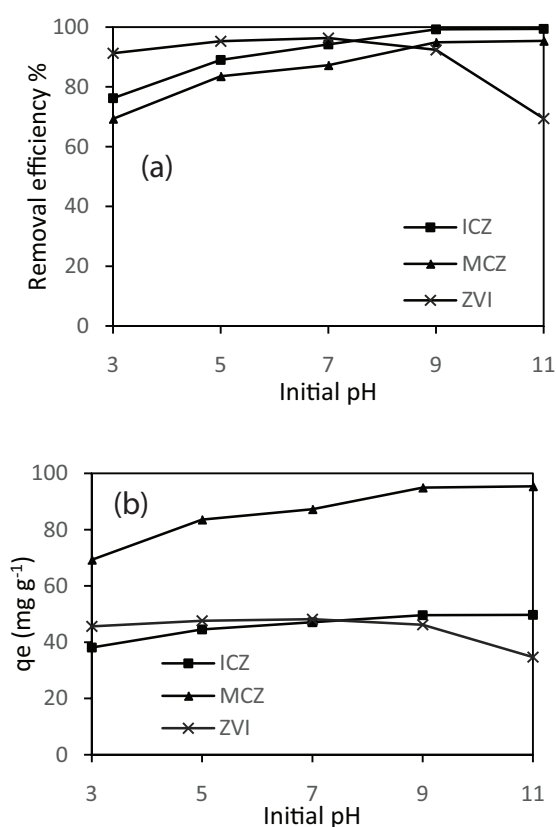

Fig. 4. Effect of initial pH on the adsorption of CV on ICZ, MCZ, and ZVI: (a) removal efficiency and (b) adsorption capacity (optimum parameters: C_0, 50 mg/L; adsorbent dosage, 1 g/L (ICZ and ZVI) and 0.5 g/L (MCZ); and agitation speed, 150 rpm).

Solution pH has been generally accepted as one of the most important factors that affect dye decolorization, because it determines the surface charge of a sorbent, the degree of ionization, and speciation of molecules or ions [32]. The adsorption ability of the surface and type of surface-active centers are indicated by the significant factor of the pH_{pzc}. The pH level on which the surface charge is zero is called pH_{pzc}, which is typically used to quantify or define the electrokinetic properties of a surface [2]. Cationic dye adsorption is favored at pH > pH_{pzc} due to presence of functional groups such as OH⁻ and COO⁻ groups. So, adsorption capacity (mg/g) tends to increase due to the electrostatic interaction between the positively charged dye and the negatively charged adsorbent (ICZ, MCZ, and ZVI) surface [33,34]. The adsorption of CV increased with an increasing pH in the adsorption onto ICZ and MCZ. The removal of CV increased from 76.24% to 99.41%, and adsorption capacities increased from 38.12 to 49.71 mg/g in the adsorption onto ICZ by increasing the pH value from 3 to 11. Similarly, the removal of CV increased from 69.29% to 95.41%, while the sorption capacities increased from 69.28 to 95.40 mg/g in the adsorption onto MCZ by increasing the pH value from 3 to 11. Similar results were previously found by Adak et al. [35] and Nandi et al. [36].

On the other hand, it was observed that by increasing the pH value from 3 to 7, the removal of CV by ZVI increased and then decreased from pH 7 to 11 as shown in Fig. 4(a). The reaction rate was pH-dependent, and the adsorption was the most effective at pH 7. The efficiency of decolorization and sorption capacity at pH 7 in equilibrium time were 96.36% and 48.18 mg/g, respectively. Sun et al. [37] noted similar results and concluded that the adsorption was favorable at higher pH, but it was depressed by the passive layer formed on the ZVI surface in alkaline conditions. In the decolorization process of aqueous CV solution by ZVI particles, the final decolorization efficiency at pH from 3 to 9 was over 90%, within 30 min of reaction time. Therefore, no pH adjustment is required for the treatment of CV-containing dye wastewater.

3.5. Effect of initial dye concentration

Figs. 5(a) and (b) show the effect of initial dye concentration (50–250 mg/L) on the adsorption of CV. The adsorption capacities of ICZ, MCZ, and ZVI increased from 49.71 to 81.87 mg/g, from 97.74 to 142.22 mg/g, and from 48.18 to 162.04 mg/g, respectively, with the increase in the initial CV concentration from 50 to 250 mg/L. The removal of CV decreased from 99.41% to 32.75%, from 97.74% to 28.44%, and from 96.36% to 64.81% in the adsorption onto ICZ, MCZ, and ZVI, respectively, with the increase in the initial CV concentration from 50 to 250 mg/L. For all adsorbents, under optimum conditions, decolorization efficiency decreased with the increase in the initial CV concentration [38,39].

3.6. Adsorption kinetics

The kinetics of the adsorption process was studied by carrying out the adsorption experiments at optimum conditions and monitoring the amount adsorbed with time. The results of the kinetics experiments are shown in Figs. 6(a) and (b).
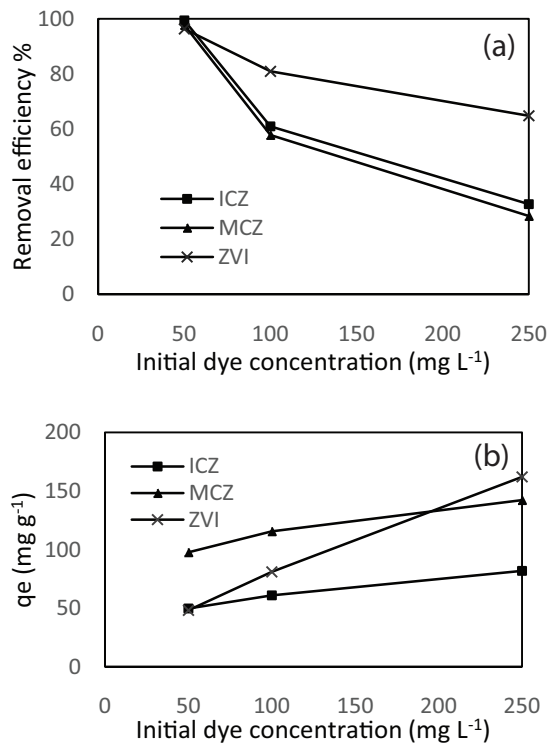
Fig. 5. Effect of initial dye concentration on the adsorption of CV on ICZ, MCZ, and ZVI: (a) removal efficiency and (b) adsorption capacity (optimum parameters: pH, 11 (ICZ and MCZ) and 7 (ZVI); adsorbent dosage, 1 g/L (ICZ and ZVI) and 0.5 g/L (MCZ); and agitation speed, 150 rpm).

The adsorption kinetics of CV removal was evaluated using pseudo-first-order, pseudo-second-order, and intra-particle diffusion models. The characteristic constants of each kinetics model were evaluated by non-linear regression using SigmaPlot software package. A low root-mean-square error (RMSE) and high R^2 specified that the kinetic models fitted the sorption process. The results are shown in Figs. 7(a)–(d).

3.6.1. Pseudo-first-order model

The pseudo-first-order equation can be described by the non-linearized form given in Eq. (5) [40]:

$$q_t = q_e\left(1 - e^{k_1 * t}\right) \tag{5}$$

where q_t (mg/g) is the amount of dye adsorbed at time t, q_e (mg/g) is the adsorption capacity at equilibrium, k_1 (min^{-1}) is the pseudo-first-order rate constant, and t (min) is the contact time.

3.6.2. Pseudo-second-order model

The pseudo-second-order equation can be described by the non-linearized form given in Eq. (6) [41]:

$$q_t = \frac{\left(k_2 \times q_e^2 t\right)}{\left(1 + k_2 \times q_e \times t\right)} \tag{6}$$
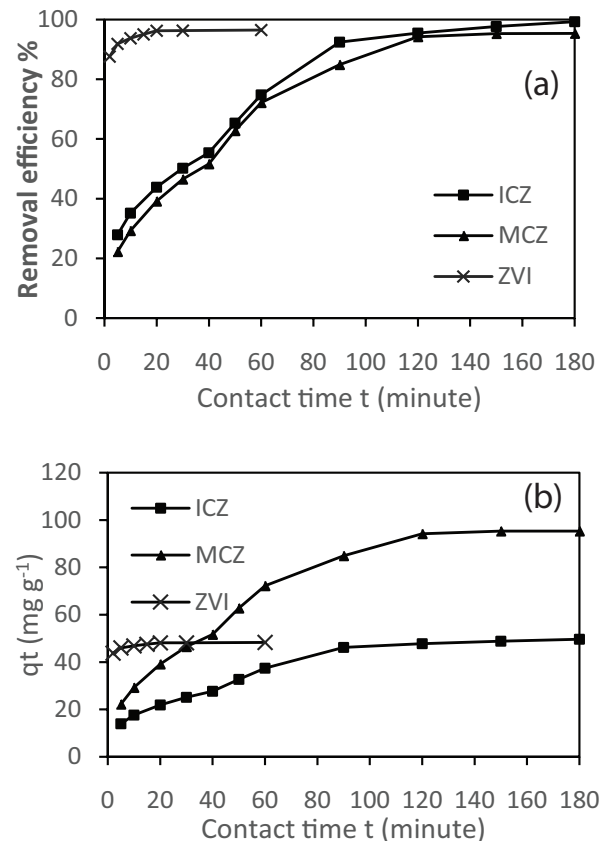

Fig. 6. Effect of contact time on the adsorption of CV on ICZ, MCZ, and ZVI: (a) removal efficiency and (b) adsorption capacity (optimum parameters: C_0, 50 mg/L; adsorbent dosage, 1 g/L (ICZ and ZVI) and 0.05 g/L (MCZ); pH, 11 (ICZ and MCZ) and 7 (ZVI); and agitation speed, 150 rpm).

where k_2 (g/mg min) is the pseudo-second-order rate constant, and q_e (mg/g) is the equilibrium sorption uptake at equilibrium time.

3.6.3. Weber–Morris intraparticle diffusion model

The intraparticle diffusion model can be described by Eq. (7) [33]:

$$q_t = k_{id} \times t^{1/2} + C \tag{7}$$

External and internal diffusions (or intraparticle diffusion) are the two stages for the adsorption process on a porous adsorbent.

An empirically found functional relationship common in most adsorption processes is that the uptake varies almost proportionally with $t^{1/2}$, and the Weber–Morris plot (q_t vs. $t^{1/2}$), rather than the contact time, t [42]:

k_{id} (mg/g min$^{-0.5}$) is the intraparticle diffusion rate constant, which can be obtained from the slope of the q_t vs. $t^{1/2}$ plot.

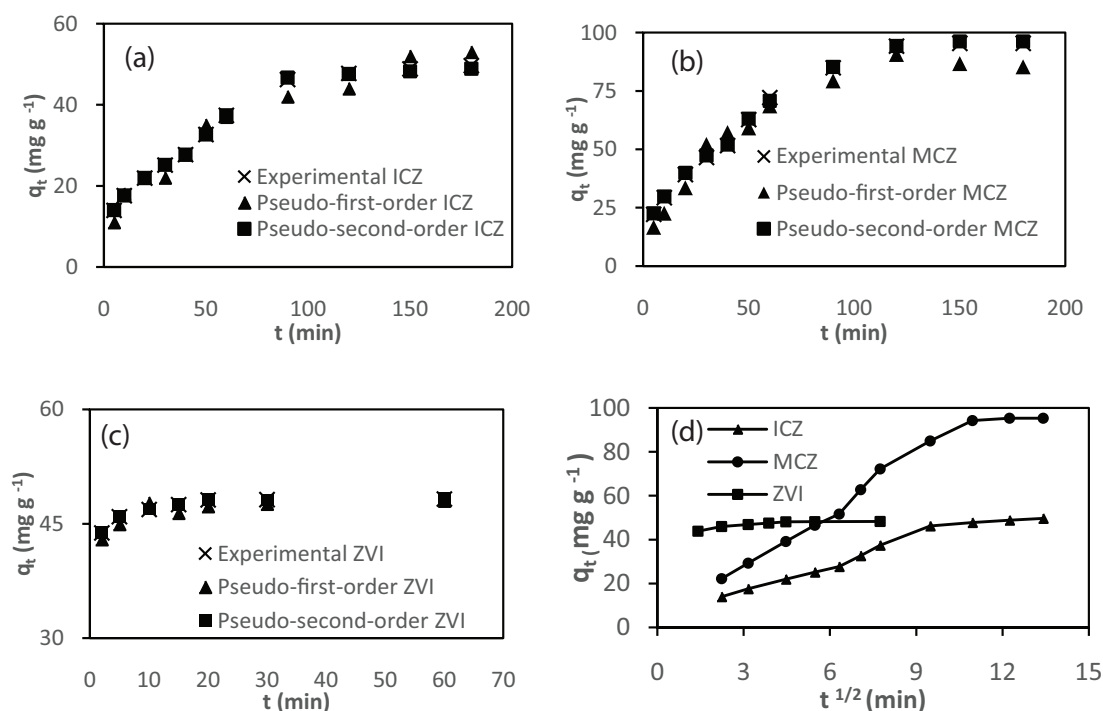The parameters that were obtained from the models are listed in Table 2.

Fig. 7. Pseudo-first-order and pseudo-second-order kinetic plots for removal of CV by (a) ICZ, (b) MCZ, (c) ZVI, and (d) intraparticle diffusions kinetic plot for removal of CV by ICZ, MCZ, and ZVI (optimum parameters: C_0, 50 mg/L; adsorbent dosage, 1 g/L (ICZ and ZVI) and 0.05 g/L (MCZ); pH, 11 (ICZ and MCZ) and 7 (ZVI); and agitation speed, 150 rpm).

Table 2
Kinetic parameters for the removal of CV by ICZ, MCZ, and ZVI

Kinetic parameters	ICZ	MCZ	ZVI
Pseudo-first order			
q_e (mg/g)	114.15	225.7	5.11
K_1 (min^{-1})	0.15	0.18	0.983
R^2	0.8324	0.9143	0.9446
RMSE	7.63	9.32	5.87
Pseudo-second order			
q_e (mg/g)	57.12	121.24	49.04
K_2 (g/mg min)	0.0024	0.0022	0.0768
R^2	0.9898	0.9901	0.9998
RMSE	2.67	3.86	3.91
Intraparticle diffusion			
k_{id}	3.5216	7.2577	0.6353
α (mg/g min)	7.08	8.56	44.39
R^2	0.9559	0.9594	0.6884
RMSE	10.89	9.65	10.76

The goodness of the fit and best model was determined using the coefficient of determination (R^2) and RMSE. A low RMSE and high R^2 specified that the kinetic models fitted the sorption process.

$$RMSE = \sqrt{\frac{1}{n}\sum(q_p - q_o)^2} \tag{8}$$

where q_p (mg/g) is the predicted sorption capacity, q_o (mg/g) is the observed sorption capacity, and n is the number of samples.

Therefore, it was concluded that pseudo-second-order kinetic model was more suitable for explaining the adsorption kinetics of CV on all adsorbents. The R^2 values were 0.9898 and 0.9901 for ICZ and MCZ, respectively. The ZVI pseudo-second-order kinetic model produced a perfect fit with the highest R^2 value of 0.9998.

3.7. Adsorption isotherms

An adsorption isotherm provides valuable information on how dye molecules are distributed between the liquid and solid phases when the adsorption process reaches an equilibrium state, which is critical in optimizing the use of adsorbents [42]. Two types of isotherm models were applied in this study—Freundlich [43] and Langmuir models [44].

The Freundlich adsorption isotherm, which assumes that adsorption takes place on heterogeneous surfaces, can be described by the non-linearized form given in Eq. (9):

$$q_e = K_F \times C_e^{1/n_F} \tag{9}$$

where q_e (mg/g) is the concentration of dye that is adsorbed, C_e (mg/L) is the equilibrium dye concentration in the aqueous solution, and K_F and n are constants that can be related to the adsorption capacity and the adsorption intensity,

respectively. The basic assumption of the Langmuir isotherm is that the sorption takes place at specific homogeneous sites within the adsorbent [33,42]. The Langmuir isotherm can be described by the non-linearized form given in Eq. (10):

$$q_e = \frac{\left(q_m \times K_L \times C_e\right)}{\left(1 + K_L \times C_e\right)} \tag{10}$$

where q_e (mg/g) is the amount adsorbed at equilibrium, C_e (mg/L) is the equilibrium concentration, q_m (mg/g) is the adsorption capacity, and K_L (L/mg) is the adsorption intensity or Langmuir coefficient.

The calculated data are shown in Figs. 8(a)–(c).

The parameters of the isotherm models' data are presented in Table 3. The characteristic constants of each isotherm model were evaluated by non-linear regression using SigmaPlot software package. A low RMSE and high R^2 specified that the isotherm models fitted the sorption process. Freundlich
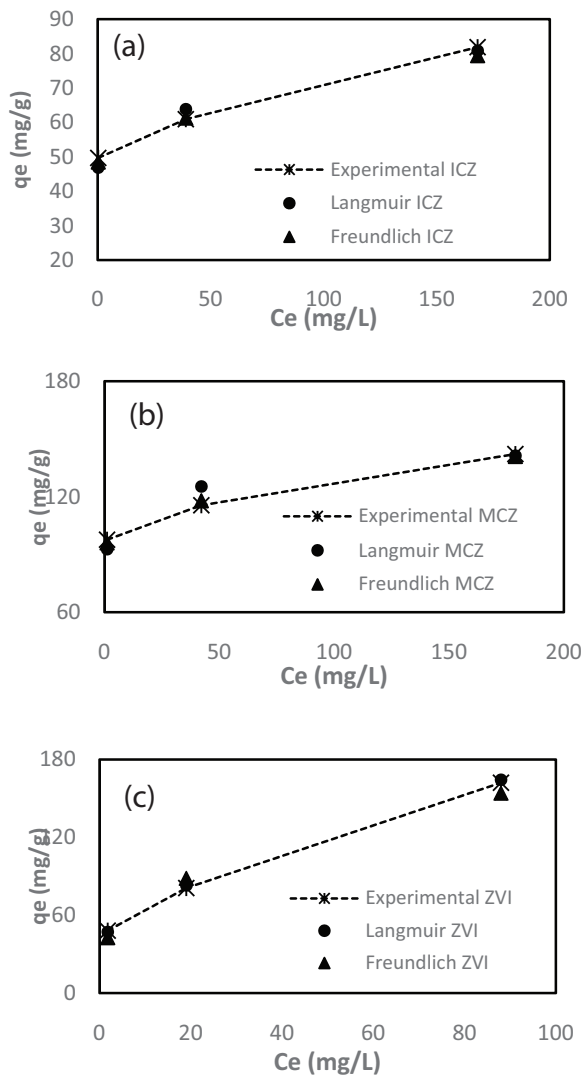

Fig. 8. Langmuir and Freundlich models for removal of CV by (a) ICZ, (b) MCZ, and (c) ZVI (optimum parameters: adsorbent dosage, 1 g/L (ICZ and ZVI) and 0.5 g/L (MCZ); pH, 11 (ICZ and MCZ) and 7 (ZVI); and agitation speed, 150 rpm).

model indicated better fitness for the adsorption of CV onto ICZ and MCZ, evidenced by the values of R^2 and RMSE. The R^2 values were respectively 0.9936 and 0.9917, which showed a good fit of this isotherm to the experimental data. This suggested a heterogeneous adsorbing surface and multilayer adsorption. Langmuir model indicated better fitness for the adsorption of CV onto ZVI. The R^2 value was 0.9954, which showed a good fit of this isotherm to the experimental data. This suggested a homogeneous adsorbing surface and monolayer adsorption. The values of q_m obtained from the Langmuir model were 81.17, 145.46, and 174.35 mg/g, for ICZ, MCZ, and ZVI, respectively.

The equilibrium parameter or the separation factor (R_L) was used to confirm the favorability of adsorption in a given concentration range, as shown in Eq. (11).

$$R_L = \frac{1}{\left(1 + K_L C_o\right)} \tag{11}$$

The value of R_L indicates the type of isotherm, which may be as follows: (1) $0 < R_L < 1$ for feasible adsorption; (2) $R_L > 1$ for unfeasible adsorption; (3) $R_L = 1$ for linear adsorption; or (4) $R_L = 0$ for irreversible adsorption [45]. The R_L values for CV adsorption on ICZ, MCZ, and ZVI were lower than 1 and greater than 0, indicating favorable adsorption. The value of n_F constant, falling in the range of 1–10, expressed a suitable adsorption process [46].

3.8. Comparison to other adsorbents

Comparisons of the adsorption capacities (q_m) of CV and basic dye are given in Table 4. It may be seen in the table that all adsorbents showed comparable adsorption capacities for CV in relevant to other adsorbents. The natural zeolite had an extremely low adsorption capacity in comparison with the modified zeolites. The results of the experiments indicated that ICZ, MCZ, and ZVI are suitable for removal of CV from an aqueous solution because they have relatively high sorption capacities.

Table 3
Langmuir and Freundlich parameters for adsorption of CV onto ICZ, MCZ, and ZVI

Isotherm parameters	ICZ	MCZ	ZVI
Langmuir			
q_m (mg/g)	81.17	145.46	174.35
K_L (L/mg)	0.142	0.214	0.071
R_L	0.123	0.09	0.727
R^2	0.9828	0.9638	0.9954
RMSE	3.56	5.81	1.57
Freundlich			
K_F (mg$^{1-1/n}$ L$^{1/n}$/g)	51.12	85.21	36.44
$1/n$	0.112	0.119	0.235
R^2	0.9936	0.9917	0.9812
RMSE	1.15	0.98	4.85

3.9. Evaluation of the synergistic effect in ZVI-MCZ and ZVI-ICZ sequential systems

Fig. 9 illustrates the synergistic effect in the ZVI-MCZ and ZVI-ICZ sequential system on CV removal at 0–60 min. In order to observe the yield better, the combined system was tested for a high concentration of CV. The experiments showed that the ZVI-ICZ sequential system could reduce about 90.36% of CV, while ZVI and ICZ by themselves could reduce 64.86% and 28.34% of CV, respectively. The ZVI-MCZ sequential system could reduce about 99.99% of CV, while ZVI and MCZ by themselves could reduce 64.86% and 24.26% of CV, respectively, in 60 min.

CV removal efficiency was increased by the ZVI-MCZ sequential addition system at pH 7, and it was observed that

Table 4
Comparison of the adsorption capacities (q_m) of various adsorbents for CV

| Adsorbents	q_m (mg/g)	References
Typha latifolia-activated carbon/ chitosan composite	2.56	[47]
Montmorillonite (Mt)	370.37	[30]
Kaolinite-supported zero-valent iron	181.8	[48]
HTS (silica with hydrotalcite)	11.2	[49]
Kaolin	47.27	[36]
Jute fiber carbon	27.99	[50]
Sawdust	37.83	[51]
Amino silica	40.0	[52]
Jackfruit leaf powder	43.39	[53]
Cu(II)-loaded montmorillonite	114.3	[54]
Rice husk	44.87	[55]
Wheat bran	80.37	[56]
Natural zeolite	55.16	[2]
ICZ	81.17	This study
MCZ	145.46	This study
ZVI	174.35	This study
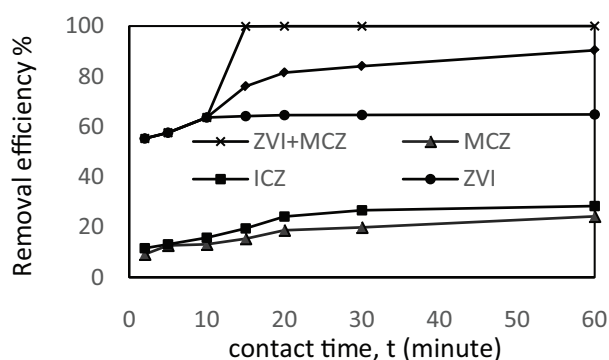
Fig. 9. Removal of CV by ZVI-MCZ and ZVI–ICZ processes (optimum parameters: initial pH, 7; C_0, 250 mg/L; adsorbent dosage, 1g/L (ZVI), 0.5 g/L (MCZ), and 1g/L (ICZ).

using ZVI and MCZ together in a sequential system could provide better removal of color than when applied separately. The combination of ZVI-MCZ enhanced the decolorization of the solutions with an increase of about 10% in comparison with the ZVI or MCZ adsorption.

Potassium permanganate ($KMnO_4$) is already being used in removal of pollutants [57,58] due to its relatively low cost and ease of handling. However, considering the undesired strong color of $KMnO_4$, only very low inlet concentration is allowed to avoid the appearance of chromaticity in the treated water [58]. It is, therefore, imperative to seek one method with low dosage of $KMnO_4$ to achieve efficient removal of dye. In recent years, the combined process has been proposed and used in wastewater treatment for removal of dye from wastewater. Wang et al. [28] attempted to use a novel synergistic technology based on ZVI and $KMnO_4$ developed for treatment of dye wastewater and achieved effective removal of MB. Zeolite, which is used as a supporting material to deposit $KMnO_4$, not only provides high active surface area but also prevents undesired color of $KMnO_4$, through formation of MCZ. Furthermore, the materials that are formed in situ by the reaction between released Fe(II) and $KMnO_4$ may enhance removal of dye. The removal efficiency of CV by Fe^0, indicated that MnO_2 could increase CV removal by Fe^0, both due to adsorption of CV by newly formed MnOOH and FeOOH and Fe^0 passivation being prevented via capturing soluble Fe(II) by MnO_2. Consequently, in the combined system of ZVI-MCZ, the CV removal time was found to be comparatively shorter than the adsorption times by MCZ and ZVI separately, and the high concentration of CV removal efficiency was more effective.

4. Conclusions

The adsorption performances of ICZ, MCZ, and ZVI particles for CV have been evaluated. Adsorption experiments were carried out as functions of contact time, adsorbent dosage, pH, and initial CV concentration. This study demonstrated that toxic CV dye molecules could be successfully removed from an aqueous solution by adsorption onto ICZ, MCZ, and ZVI. The isotherms of the adsorption of CV dye molecules onto ICZ and MCZ were best described by the Freundlich model. The adsorption isotherm onto ZVI was described better by the Langmuir isotherm. The kinetics of the adsorption of CV dye molecules onto ICZ, MCZ, and ZVI was best described by the pseudo-second-order model, which means that the rate-limiting step may be chemical sorption rather than diffusion. The results showed that the adsorption efficiency of CV dye molecules onto MCZ was higher than that of ICZ and ZVI, but the adsorption of CV onto ZVI particles was faster than that onto ICZ and MCZ. ICZ and MCZ exhibited the best performance at pH 11, while ZVI exhibited the best performance at pH 7.

This study showed the possibility of using ICZ, MCZ, and ZVI as nanoparticles, an alternative for the adsorbents that are already being used, in the removal of CV from industrial wastewater as. Furthermore, the combination of ZVI-MCZ enhanced the decolorization of the solutions. The best result was found with the ZVI-MCZ sequential system.

References

[1] S. Dawood, T.K. Sen, Removal of anionic dye Congo red from aqueous solution by raw pine and acid-treated pine cone powder as adsorbent: equilibrium, thermodynamic, kinetics, mechanism and process design, Water Res., 46 (2012) 1933–1946.

[2] M.T. Yagub, T.K. Sen, S. Afroze, H.M. Ang, Dye and its removal from aqueous solution by adsorption: a review, Adv. Colloid Interface Sci., 209 (2014) 172–184.

[3] T. Madrakian, A. Afkhami, H. Mahmood-Kashani, M. Ahmadi, Adsorption of some cationic and anionic dyes on magnetite nanoparticles-modified activated carbon from aqueous solutions: equilibrium and kinetics study, J. Iran. Chem. Soc., 10 (2013) 481–489.

[4] K.P. Singh, S. Gupta, A.K Singh, S. Sinha, Optimizing adsorption of crystal violet dye from water by magnetic nanocomposite using response surface modeling approach, J. Hazard. Mater., 186 (2011) 1462–1473.

[5] R. Kumar, R. Ahmad, Biosorption of hazardous crystal violet dye from aqueous solution onto treated ginger waste (TGW), Desalination, 265 (2011) 112–118.

[6] A. Saeed, M. Sharif, M. Iqbal, Application potential of grapefruit peel as dye sorbent: kinetics, equilibrium and mechanism of crystal violet adsorption, J. Hazard. Mater., 179 (2010) 564–572.

[7] S. Khansorthong, M. Hunsom, Remediation of wastewater from pulp and paper mill industry by the electrochemical technique, Chem. Eng. J., 151 (2009) 228–234.

[8] M.K. Purkait, S. DasGupta, S. De, Micellar enhanced ultrafiltration of eosin dye using hexadecyl pyridinium chloride, J. Hazard. Mater., 136 (2006) 972–977.

[9] B. Gözmen, B. Kayan, A.M. Gizir, A. Hesenov, Oxidative degradations of reactive blue 4 dye by different advanced oxidation methods, J. Hazard. Mater., 168 (2009) 129–136.

[10] W. Zou, R. Han, Z. Chen, Z. Jinghua, J. Shi, Kinetic study of adsorption of Cu(II) and Pb(II) from aqueous solutions using manganese oxide coated zeolite in batch mode, Colloids Surf., A, 279 (2006) 238–246.

[11] V. Meshko, L. Markovska, M. Mincheva, A.E. Rodrigues, Adsorption of basic dyes on granular activated carbon and natural zeolite, Water Res., 35 (2001) 3357–3366.

[12] B. Armağan, M. Turan, M.S. ęlik, Equilibrium studies on the adsorption of reactive azo dyes into zeolite. Desalination 170 (2004) 33-39.

[13] O. Ozdemir, B. Armagan, M. Turan, M.S. Çelik, Comparison of the adsorption characteristics of azo-reactive dyes on mezoporous minerals, Dyes Pigm., 62 (2004) 49–60.

[14] K.Y. Hor, J.M.C. Chee, M.N. Chong, B. Jin, C. Saint, P.E. Poh, R. Aryal, Evaluation of physicochemical methods in enhancing the adsorption performance of natural zeolite as low-cost adsorbent of methylene blue dye from wastewater, J. Cleaner Prod., 118 (2016) 197–209.

[15] S. Liu, Y. Ding, P. Li, K. Diao, X. Tan, F. Lei, Y. Zhan, Q. Li, B. Huang, Z. Huang, Adsorption of the anionic dye Congo red from aqueous solution onto natural zeolites modified with *N,N*-dimethyl dehydroabietylamine oxide, Chem. Eng. J., 248 (2014) 135–144.

[16] L.B. Far, B. Souri, M. Heidari, R. Khoshnavazi, Evaluation of iron and manganese-coated pumice application for the removal of as(v) from aqueous solutions, Iran. J. Environ. Health Sci. Eng., 9 (2012) 21.

[17] S. Ezati, B. Souri, A. Maleki, Evaluation of iron-coated ZSM-5 zeolite for removal of As(III) from aqueous solutions in batch and column systems, Water Sci. Technol. Water Supply, 17 (2017) 10–23.

[18] E. Eren, O. Cubuk, H. Ciftci, B. Eren, B. Caglar, Adsorption of basic dye from aqueous solutions by modified sepiolite: equilibrium, kinetics and thermodynamics study, Desalination, 252 (2010) 88–96.

[19] L.N. Zou, Y.F. Xu, X.H. Ma, J.Y. Ma and R.P. Han: Adsorption of methylene blue and copper ions from aqueous solutions by iron-oxide-coated-zeolite, J. Zhengzhou Uni.(Sci. Ed.), 41(3) (2009) 78–84.

[20] L. Zhao, W. Zou, L. Zou, X. He, J. Song, R. Han, Adsorption of methylene blue and methyl orange from aqueous solution by iron oxide-coated zeolite in fixed bed column: predicted curves, Desal. Wat. Treat., 22 (2010) 258–264.

[21] S.A. Dastgheib, T. Karanfil, W. Cheng, Tailoring activated carbons for enhanced removal of natural organic matter from natural waters, Carbon, 42 (2004) 547–557.

[22] C.H. Lai, C.Y. Chen, Removal of metal ions and humic acid from water by iron-coated filter media, Chemosphere, 44 (2001) 1177–1184.

[23] C.H. Lai, S.L. Lo, H.L. Chiang, Adsorption/desorption properties of copper ions on the surface of iron-coated sand using BET and EDAX analyses, Chemosphere, 41 (2000) 1249–1255.

[24] M. Kitis, S.S. Kaplan, E. Karakaya, N.O. Yigit, G. Civelekoglu, Adsorption of natural organic matter from waters by iron coated pumice, Chemosphere, 66 (2007) 130–138.

[25] D. Gümüş, F. Akbal, A comparative study of ozonation, iron coated zeolite catalyzed ozonation and granular activated carbon catalyzed ozonation of humic acid, Chemosphere, 174 (2017) 218–231.

[26] S.R. Taffarel, J. Rubio, On the removal of Mn^{2+} ions by adsorption onto natural and activated Chilean zeolites, Miner. Eng., 22 (2009) 336–343.

[27] S.R. Taffarel, J. Rubio, Removal of Mn^{2+} from aqueous solution by manganese oxide coated zeolite, Miner. Eng., 23 (2010) 1131–1138.

[28] X. Wang, P. Liu, M. Fu, J. Ma, P. Ning, Novel sequential process for enhanced dye synergistic degradation based on nano zero-valent iron and potassium permanganate, Chemosphere, 155 (2016) 39–47.

[29] M.E. Summer, Effect of iron oxides on positive and negative charges in clays and soils, Clay Miner. Bull., 5 (1963) 218–226.

[30] G.K. Sarma, S.S. Gupta, K.G. Bhattacharyya, Adsorption of Crystal violet on raw and acid-treated montmorillonite, K10, in aqueous suspension, J. Environ. Manage., 171 (2016) 1–10.

[31] M. Iqbal, N. Iqbal, I.A. Bhatti, N. Ahmad, M. Zahid, Response surface methodology application in optimization of cadmium adsorption by shoe waste: a good option of waste mitigation by waste, Ecol. Eng., 88 (2016) 265–275.

[32] U.A. Guler, M. Ersan, E. Tuncel, F. Dügenci, Mono and simultaneous removal of crystal violet and safranin dyes from aqueous solutions by HDTMA-modified *Spirulina* sp., Process Saf. Environ. Prot., 99 (2016) 194–206.

[33] Z.M. Hussin, N. Talib, N.M. Hussin, M.A.K.M. Hanafiah, W.K.A.W.M. Khalir, Methylene blue adsorption onto NaOH modified durian leaf powder: isotherm and kinetic studies, Am. J. Environ. Eng., 5 (2015) 38–43.

[34] A.E. Pirbazari, E. Saberikhah, M. Badrouh, M.S. Emami, Alkali treated Foumanat tea waste as an efficient adsorbent for methylene blue adsorption from aqueous solution, Water Res. Ind., 6 (2014) 64–80.

[35] A. Adak, M. Bandyopadhyay, A. Pal, Removal of crystal violet dye from wastewater by surfactant-modified alumina, Sep. Purif. Technol., 44 (2005) 139–44.

[36] B.K. Nandi, A. Goswami, A.K. Das, B. Mondal, M.K. Purkait, Kinetic and equilibrium studies on the adsorption of crystal violet dye using kaolin as an adsorbent, Sep. Sci. Technol., 43 (2008) 1382–1403.

[37] X. Sun, T. Kurokawa, M. Suzuki, M. Takagi, Y. Kawase, Removal of cationic dye methylene blue by zero-valent iron: effects of pH and dissolved oxygen on removal mechanisms, J. Environ. Sci. Health Part A Toxic/Hazard. Subst. Environ. Eng., 50 (2015) 1057–1071.

[38] A.R. Tehrani-Bagha, H. Nikkar, N.M. Mahmoodi, M. Markazi, F.M. Menger, The sorption of cationic dyes onto kaolin: kinetic, isotherm and thermodynamic studies, Desalination, 266 (2011) 274–280.

[39] F. Akbal, Adsorption of basic dyes from aqueous solution onto pumice powder, J. Colloid Interface Sci., 286 (2005) 455–458.

[40] S. Lagergren, Zur theorie der sogenannten adsorption gelöster stoffe, K. Sven, Vetenskapsakad. Handl., 24 (1898) 1–39.

[41] Y.-S. Ho, Review of second-order models for adsorption systems, J. Hazard. Mater., 136 (2006) 681–689.

[42] S. Kaur, S. Rani, R.K. Mahajan, M. Asif, V.K. Gupta, Synthesis and adsorption properties of mesoporous material for the removal of dye safranin: kinetics, equilibrium, and thermodynamics, J. Ind. Eng. Chem., 22 (2015) 19–27.

[43] H.M.F. Freundlich, Uber die adsorption in lasungen, Z. Phys. Chem., 57 (1906) 385–470.

[44] I. Langmuir, The constitution and fundamental properties of solids and liquids. Part I. Solids, J. Am. Chem. Soc., 38 (1916) 2221–2295.

[45] H. Mahmoodian, O. Moradi, B. Shariatzadeha, T.A. Salehf, I. Tyagi, A. Maity, M. Asif, V.K. Gupta, Enhanced removal of methyl orange from aqueous solutions by poly HEMA–chitosan-MWCNT nano-composite, J. Mol. Liq., 202 (2015) 189–198.

[46] A. Keranen, T. Leiviska, O. Hormi, J. Tanskanen, Removal of nitrate by modified pine sawdust: effects of temperature and co-existing anions, J. Environ. Manage., 147 (2015) 46–54.

[47] H.J. Kumari, P. Krishnamoorthy, T.K. Arumugam, S. Radhakrishnan, D. Vasudevan, An efficient removal of crystal violet dye from waste water by adsorption onto TLAC/Chitosan composite: a novel low cost adsorbent, Int. J. Biol. Macromol., 96 (2017) 324–333.

[48] Z. Chen, T. Wang, X. Jin, Z. Chen, M. Megharaj, R. Naidu, Multifunctional kaolinite-supported nanoscale zero-valent iron used for the adsorption and degradation of crystal violet in aqueous solution, J. Colloid Interface Sci., 398 (2013) 59–66.

[49] Y.F. Tao, W.G. Lin, L. Gao, J. Yang, Y. Zhou, J.Y. Yang, F. Wei, Y. Wang, J.H. Zhu, Low-cost and effective phenol and basic dyes trapper derived from the porous silica coated with hydrotalcite gel, J. Colloid Interface Sci., 358 (2011) 554–561.

[50] K. Porkodi, K.V. Kumar, Equilibrium, kinetics and mechanism modeling and simulation of basic and acid dyes sorption onto jute fiber carbon: eosin yellow, malachite green and crystal violet single component systems, J. Hazard. Mater., 143 (2007) 311–327.

[51] H. Parab, M. Sudersanan, N. Shenoy, T. Pathare, B. Vaze, Use of agro-industrial wastes for removal of basic dyes from aqueous solutions, Clean Soil Air Water, 37 (2009) 963–969.

[52] H. Yang, D. Zhou, Z. Chang, L. Zhang, Adsorption of crystal violet onto amino silica: optimization, equilibrium, and kinetic studies, Desal. Wat. Treat., 52 (2014) 6113–6121.

[53] P.D. Saha, S. Chakraborty, S. Chowdhury, Batch and continuous (fixed-bed column) biosorption of crystal violet by *Artocarpus heterophyllus* (jackfruit) leaf powder, Colloids Surf., B, 92 (2012) 262–270.

[54] X.S. Wang, W. Zhang, Removal of basic dye crystal violet from aqueous solution by Cu (II)-loaded montmorillonite, Sep. Sci. Technol., 46 (2011) 656–663.

[55] S. Chakraborty, S. Chowdhury, P.D. Saha, Adsorption of Crystal Violet from aqueous solution onto NaOH-modified rice husk, Carbohydr. Polym., 86 (2011) 1533–1541.

[56] X.S. Wang, X. Liu, L. Wen, Y. Zhou, Y. Jiang, Z. Li, Comparison of basic dye crystal violet removal from aqueous solution by low-cost biosorbents, Sep. Sci. Technol., 43 (2008) 3712–3731.

[57] X.R. Xu, H.B. Li, W.H. Wang, J.D. Gu, Decolorization of dyes and textile wastewater by potassium permanganate, Chemosphere, 59 (2005) 893–898.

[58] J. Zhang, B. Sun, X.M. Xiong, N.Y. Gao, W.H. Song, E.D. Du, X.H. Guan, G.M. Zhou, Removal of emerging pollutants by Ru/TiO$_2$–catalyzed permanganate oxidation, Water Res., 63 (2014) 262–270.